HSP90 and eNOS partially co-localize and change cellular localization in relation to different ECM components in 2D and 3D cultures of adult rat cardiomyocytes

Article *in* Biology of the Cell · January 2008

DOI: 10.1042/BC20070043 · Source: PubMed

9 authors, including:

Valentina Di Felice
Università degli Studi di Palermo
52 PUBLICATIONS **559** CITATIONS
SEE PROFILE

Francesco Cappello
University of Palermo, Palermo, Italy
274 PUBLICATIONS **3,368** CITATIONS
SEE PROFILE

Angela De Luca
Istituto Ortopedico Rizzoli
15 PUBLICATIONS **121** CITATIONS
SEE PROFILE

Filippo Macaluso
Università degli Studi eCampus
40 PUBLICATIONS **282** CITATIONS
SEE PROFILE

Biol. Cell (2007) **99**, 689–699 (Printed in Great Britain) doi:10.1042/BC20070043

Research article

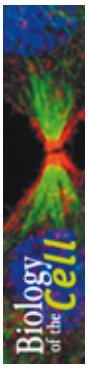

HSP90 and eNOS partially co-localize and change cellular localization in relation to different ECM components in 2D and 3D cultures of adult rat cardiomyocytes

Valentina Di Felice*[1], Francesco Cappello*, Antonella Montalbano*, Nella Maria Ardizzone*, Angela De Luca*, Filippo Macaluso*, Daniela Amelio†‡, Maria Carmela Cerra†‡ and Giovanni Zummo*

* Human Anatomy Section 'E. Luna', Department of Experimental Medicine, University of Palermo, Via del Vespro 129, 90127 Palermo, Italy, †Department of Pharmaco-Biology, University of Calabria, 87030 Arcavacata di Rende, CS, Italy, and ‡Department of Cellular Biology, University of Calabria, 87030 Arcavacata di Rende, CS, Italy

Background information. Cultivation techniques promoting three-dimensional organization of mammalian cells are of increasing interest, since they confer key functionalities of the native ECM (extracellular matrix) with a power for regenerative medicine applications. Since ECM compliance influences a number of cell functions, Matrigel-based gels have become attractive tools, because of the ease with which their mechanical properties can be controlled. In the present study, we took advantage of the chemical and mechanical tunability of commonly used cell culture substrates, and co-cultures to evaluate, on both two- and three-dimensional cultivated adult rat cardiomyocytes, the impact of ECM chemistry and mechanics on the cellular localization of two interacting signalling proteins: HSP90 (heat-shock protein of 90 kDa) and eNOS (endothelial nitric oxide synthase).

Results. Freshly isolated rat cardiomyocytes were cultured on fibronectin, Matrigel gel or laminin, or in co-culture with cardiac fibroblasts, and tested for both integrity and viability. As validation criteria, integrity of both plasma membrane and mitochondria was evaluated by transmission electron microscopy. Cell sensitivity to microenvironmental stimuli was monitored by immunofluorescence and confocal microscopy. We found that HSP90 and eNOS expression and localization are affected by changes in ECM composition. Elaboration of the images revealed, on Matrigel-cultured cardiomyocytes, areas of high co-localization between HSP90 and eNOS and co-localization coefficients, which indicated the highest correlation with respect to the other substrates.

Conclusions. Our three-dimensional adult cardiomyocyte cultures are suitable for both analysing cell–ECM interactions at electron and confocal microscopy levels and monitoring micro-environment impact on cardiomyocyte phenotype.

[1]To whom correspondence should be addressed (email valentina.difelice@unipa.it).

Key words: artificial extracellular matrix, cardiomyocyte, co-culture, confocal microscopy, electron microscopy, protein co-localization.

Abbreviations used: 2D, 3D, two- and three-dimensional; ECM, extracellular matrix; eNOS, endothelial nitric oxide synthase; FBS, foetal bovine serum; HSP90,heat-shock protein of 90 kDa; M_1, Mander's co-localization split coefficient for channel 1; M_2, Mander's co-localization split coefficient for channel 2; R, Mander's overlap coefficient; R_r, Pearson's correlation coefficient; SEM, scanning electron microscopy; TEM, transmission electron microscopy.

Introduction

The potential of tissue engineering has become particularly attractive in the context of cardiovascular tissues, as documented by significant research over the past two decades (Niklason, 1999; Nerem and Seliktar, 2001). However, the majority of approaches have proved inadequate to yield functional cardiovascular tissues, revealing that, in comparison

with the 2D (two-dimensional) cell cultures, 3D (three-dimensional) engineered tissue constructs represent more realistic *in vitro* models (Griffith and Naughton, 2002). Cardiomyocytes are highly differentiated non-dividing immobile cells (Eisenberg and Eisenberg, 2004). Because of their characteristics, it is difficult to isolate them from the adult heart, and after isolation they have a short life *in vitro*. Adult differentiated cardiomyocytes were isolated for the first time in 1983 by a few research groups, including Jacobson et al. (1983) and Nag et al. (1983). Although these electrically excitable and spontaneously beating cells were maintained up to 45 days in culture, most of them exhibited prominent alterations in their external and internal structural organization (Nag et al., 1983). From these early studies the isolation of adult cardiomyocytes gradually became a mainstream physiological research activity, involving, for example, the assessment of monophasic action potentials using intracellular microelectrodes. During the past few years many attempts have been made to generate a cell culture system in which cell–ECM (extracellular matrix) interactions, and the stretch forces generated by membrane proteins in the heart tissue microenvironment, could be studied appropriately (Imanaka-Yoshida et al., 1999; VanWinkle et al., 2002). It has been recognized that *in vivo* cardiomyocytes adhere to the ECM by means of integrin-, cadherin- and syndecan-adhesion complexes (Matsushita et al., 1999). The discovery of the role of costameres, which form a proteic complex between vinculin, Z-lines and plasma membrane, provides a novel insight into the molecular and ultrastructural mechanisms responsible for the transmission of contraction forces from myofibrils to ECM (Sharp et al., 1997).

In addition to other reasons, the need for a 3D cell culture system originates from artifacts produced by monolayer cultures characterized by a free dorsal cellular surface, which does not exist in the myocardial architecture *in vivo*. This is epitomized by the N-cadherin-containing costameres that appear to be involved in myofibrillogenesis on this free dorsal surface, whereas in the cardiac muscle they are localized at the lateral sarcolemma in association with α-actinin and α- and β-catenin (Wu et al., 2002). An alternative to monolayer cultures is represented by ECM-embedded cells or collagen gels (Willey et al., 2003), which are covered by a thin ECM layer and may also develop cell–ECM contacts on the upper surface. The introduction of specific plastic devices has permitted the development of the 3D culture system and, consequently, a novel strategy for analysing cell–ECM interactions using TEM (transmission electron microscopy), confocal microscopy and tissue engineering. Van Luyn et al. (2002) stressed the importance of ECM components on cell function comparing 2D-with 3D-cultivated cardiomyocytes. They demonstrated that 2D fibronectin-cultured cells beat for up to 135 days, but displayed the presence of desynchronized beating. In contrast, although surviving for only 28 days, 3D collagen-cultivated cells contract simultaneously and in unison with the ECM (van Luyn et al., 2002).

The goal of the present study was to generate a 3D biocompatible alternative to monolayer cultures that is suitable to study the impact of ECM mechanics through the evaluation of expression and cellular localization of the two members of the cardiac NO signalling pathway proteins, HSP90 (heat-shock protein of 90 kDa) and eNOS (endothelial nitric oxide synthase). By developing a rapid method to isolate cardiomyocytes from adult rat heart, we cultured them two-dimensionally, on either fibronectin or laminin, or three-dimensionally, either submerged into an artificial ECM or in co-culture with cardiac fibroblasts obtained from the same heart. Using confocal microscopy, we evaluated the expression and the cellular co-localization of HSP90, a chaperone involved also in focal adhesion formation through interaction with ILK (β1-integrin-associated protein kinase) (Aoyagi et al., 2005) and eNOS, an HSP90-interacting protein. We focused on these two proteins as markers of cardiomyocyte viability for several reasons. First, it is well known that their reciprocal interaction plays a leading role in signal transduction within intact *in vivo* cardiomyocytes (Garcia-Cardena et al., 1998). HSP90, in addition to its scaffolding roles, regulates eNOS phosphorylation status, and thus enzymatic eNOS-dependent NO production. Secondly, co-ordinated changes in their expression that occur under pathological conditions, such as ischaemia/reperfusion and hypertrophy, represent compensatory mechanisms to preserve an appropriate nitrergic control of cardiomyocyte function (Piech et al., 2003; Kupatt et al., 2004). Lastly, we are using these signalling proteins in our ongoing

research regarding the interaction between extracellular endocrine stimuli (i.e. chromogranin A-derived peptides) and cardiomyocytes (Tota et al., 2007).

Our results demonstrated that cardiomyocytes cultured in a 3D Matrigel exhibit features similar to native tissue and that the mechanical properties of 2D and 3D cell culture substrates influence HSP90 and eNOS expression and cellular localization.

Results

3D co-cultures and artificial ECM cultures of adult rat cardiomyocytes

Rod-shaped cardiomyocytes and cells of different types were obtained from the cellular preparation. Non-adherent cells were cardiomyocytes (Figure 1A) and adherent cells were cardiac fibroblasts (Figure 1B). Cardiomyocytes and cardiac fibroblasts were easily isolated from the cellular suspension, because they represented 80% of non-adherent cells and 90% of adherent cells respectively. Cardiac fibroblasts isolated from the same heart were used for 3D co-cultures, and isolated cardiomyocytes were used for monolayer and 3D cultures.

The morphology of 3D co-cultured cardiomyocytes was studied by SEM (scanning electron microscopy) 3–4 days after isolation (Figure 1C), showing the external surface of isolated cardiomyocytes co-cultured with either cardiac fibroblasts (Figure 1C) or on a fibronectin layer (Figure 1D). Cardiomyocytes appeared as rod-shaped isolated cells with their myofibrils visible beneath the plasma membrane (Figures 1C and 1D). Cardiac fibroblasts produced cell–cell contacts over the cardiomyocyte plasma membrane, recurrently forming an envelope on the cardiomyocyte surface (Figure 1C). Cardiomyocytes cultured on a fibronectin layer (Figure 1D) did not show any interaction with the substrate, remaining on the insert surface as immobile low-interacting cells. Cardiomyocytes cultured on laminin showed the same morphology as fibronectin monolayer cultures (data not shown). Matrigel cultures are not suitable for SEM, thus morphology was studied by TEM analysis instead.

Semi-thin sections of TEM samples showed cardiomyocytes embedded into 3D Matrigel cultures (Figures 1E and 1F). TEM analysis of 3D Matrigel cardiomyocyte cultures showed details of myocardial cells, which were preserved despite the use of L.R. White resin (Figures 2A and 2B). Mitochondria were the most distinguishable elements and, due to their crucial intracellular function, they were used as controls of cellular viability (Figures 2A and 2B). Other cellular components, for example, myofibrils (Figure 2A) and membranes (Figure 2B), were also visible and distinguishable. Many cardiomyocytes maintained their myofibril organization, which otherwise is lost when isolated from the heart tissue (Figure 2A). Due to the difficulty of isolating pure cardiomyocytes, some fibroblasts remained in culture. In Figure 2(B), small dark strips, identified as collagen type I, were visible outside the cell in the interstitial space (Figure 2B).

Cardiomyocyte cell spreading in 3D Matrigel cultures

We systematically assessed the cell area of cardiomyocytes on longitudinal sections of 3D cultures and heart tissue as a function of cell adhesion to ECM and Matrigel mechanical properties (Peyton et al., 2006). The histogram (Figure 1G) reveals that in Matrigel the majority of the cardiomyocytes has a slightly smaller area than in the heart tissue. However, the statistical analysis of cell area distribution of both data groups revealed that the two samples matched the same model of distribution, the geometric one, with a $P < 0.005$. Conceivably, the same type of distribution for both groups suggests that the behaviour of cardiomyocytes either in Matrigel or in the native tissue is similar.

HSP90α/β and eNOS expression in 3D and 2D culture models

Unlike traditional light microscopy, confocal laser-scanning microscopy allowed the study, in a 3D manner, of the cellular distribution of the two related proteins HSP90 and eNOS. To study the influence of different substrates on the expression of the two proteins, four different matrices were used: cardiac fibroblasts, fibronectin, Matrigel gel and laminin (Figure 3). In particular, we compared 2D with 3D cultures and the effect of different compounds on the expression of the two proteins. Figure 3 shows the expression and co-localization of HSP90 and eNOS. When the cardiomyocytes were cultivated embedded either in Matrigel (Figures 3I–3M), or over a layer of laminin (Figures 3O–3Q), a high level of expression

Figure 1 | Isolation of adult rat cardiomyocytes and preparation of 3D cultures

(**A**) Freshly isolated cardiomyocytes under phase-contrast microscopy. (**B**) Freshly isolated cardiac fibroblasts, obtained from the same myocardium, under phase-contrast microscopy. (**C**) SEM of 3D co-cultures of cardiomyocytes and cardiac fibroblasts on a BD Falcon insert. (**D**) Isolated cardiomyocytes cultured in a BD Falcon insert over a layer of fibronectin; SEM. (**E**, **F**) Semi-thin sections for the TEM preparation of 3D cultures of cardiomyocytes in Matrigel. (**G**) The distribution of cardiomyocyte spreading was determined for both 3D Matrigel cultures (white bars) and heart tissue (hatched bars). The statistical distribution model was calculated with the Statistica 6.0 application and represented in the histogram (3D Matrigel cultures = hatched bar, $P = 0.0027$; heart tissue=continous line; $P = 0.0016$).

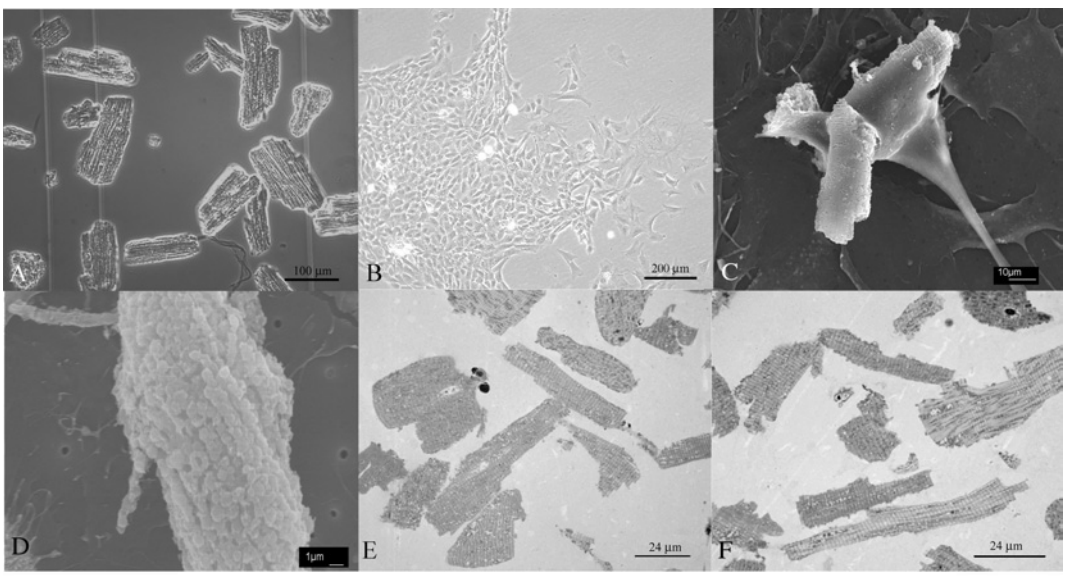

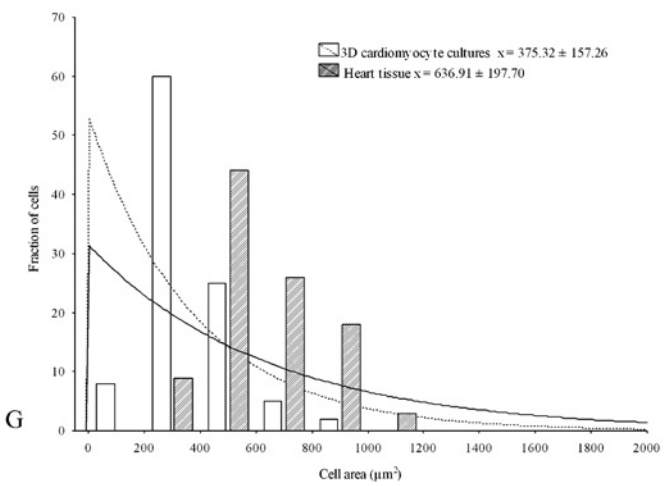

of both proteins was detected. In both cell cultures HSP90 protein appeared widely spread over the cell, without a specific cellular localization. In contrast, eNOS signal was mainly located at the boundaries of the cell, probably at the membrane level, and to a less extent in the middle of the cell. When cardiomyocytes were cultivated on fibronectin (Figures 3E–3G), or in co-culture with cardiac fibroblasts (Figures 3A–3C), both HSP90 and eNOS were poorly expressed, small spots of expression being localized within the cell. In addition, on myocytes co-cultured on fibroblasts, a definite HSP90 and eNOS signal outlined the cells. However, because of the concurrent presence of both cardiomyocytes and fibroblasts, it is not

Figure 2 | TEM micrographs of 3D Matrigel cultures of adult rat cardiomyocytes showing the integrity of myofibrils, mitochondria, plasma membrane and native ECM

(**A**) Myofibrils (m) and mitochondria (mt) inside a cultured cardiomyocyte; (**B**) two facing plasma membranes (pm), one belonging to the cardiomyocyte (card) to the left and one belonging to the fibroblast (fb) to the right. In the extracellular space, between the two cells, native ECM (ecm) was visible as thin dark strips compared with the colourless artificial ECM (data not shown).

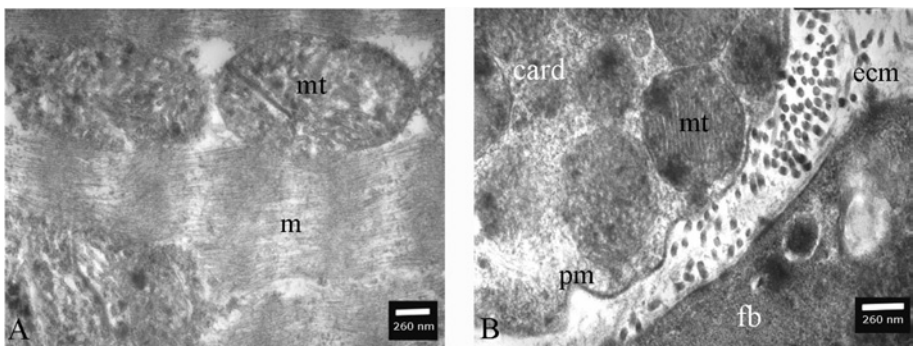

possible to distinguish in which cell the signal is located. The interferential diffraction pictures showed the shape and integrity of the cells during confocal microscopy observation (Figures 3D, 3H, 3N and 3R).

To reveal the presence and the distribution of areas of co-localization, we analysed two images using ImageJ for each substrate (HSP90 in green and eNOS in red) and we obtained four images. Two of them showed HSP90 and eNOS localization after background removal for both the red and green channel respectively (data not shown), and confirmed the distribution pattern obtained with the confocal observation. A third image was an overlay representation of both the red and green signals (Figures 4A, 4C, 4E and 4G), and a fourth pseudocolour PDM (product of differences from the mean) image indicates the areas of high and low co-localization in yellow and in blue respectively, and in black the areas where there was not any correlation at all between the expression of the two proteins (Figures 4B, 4D, 4F and 4H). The co-localization images of cardiomyocytes cultured with either cardiac fibroblasts or on fibronectin were characterized by a prevalent black colour, and by small yellow areas which were indicative of a spatially restricted, but highly correlated, expression of the two proteins (Figures 4B and 4D). In contrast, images of cardiomyocytes cultured on both Matrigel and laminin showed large blue sarcolemmal areas of low correlation and numerous yellow areas of high correlation in the central region (Figures 4F and 4H). Application of the intensity correlation analysis plug-in, which provided all co-localization coefficients (Table 1) for each culture condition, allowed a quantitative description of the various co-localization patterns. Cardiomyocytes co-cultured on fibroblasts revealed that the small areas of co-localization were characterized by a high correlation indicated by R_r (Pearson's correlation coefficient) = 0.548 and R (Mander's overlap coefficient) = 0.881, M_1 (Mander's co-localization split coefficient for channel 1) = 0.767 and M_2 (Mander's co-localization split coefficient for channel 2) = 0.605. Also in the case of fibronectin-cultured cells the coefficients were very high ($R_r = 0.621$, $R = 0.825$, $M_1 = 0.625$ and $M_2 = 0{,}499$), but the resulting image was almost black due to the very low expression of the two proteins. Remarkably, cardiomyocytes cultured on both Matrigel and laminin showed a different pattern. With respect to the other substrates, lower Pearson's correlation coefficients were found ($R_{r\ \mathrm{Matrigel}} = 0.341$ and $R_{r\ \mathrm{laminin}} = 0.121$). However, the overlap R coefficients were very similar to those obtained with the other substrates ($R_{\mathrm{Matrigel}} = 0.833$ and $R_{\mathrm{laminin}} = 0.697$). Evaluation of Mander's split coefficients ($M_{1\ \mathrm{Matrigel}} = 0.975$, $M_{2\ \mathrm{Matrigel}} = 0.87$, $M_{1\ \mathrm{laminin}} = 0.599$ and $M_{2\ \mathrm{laminin}} = 0.8$) revealed that the highest degree of HSP90 and eNOS co-localization was present on Matrigel cultures.

Figure 3 | Confocal analysis of HSP90 and eNOS co-localization

Confocal laser images showing HSP90α/β (green) and eNOS (red) expression and their co-localization in adult rat cardiomyocytes cultured in co-culture with cardiac fibroblasts (**A**–**C**), or on fibronectin (**E**–**G**), Matrigel (**I**–**M**) or laminin (**O**–**Q**). (**D**, **H**, **N**, **R**) show cell integrity with differential interference contrast.

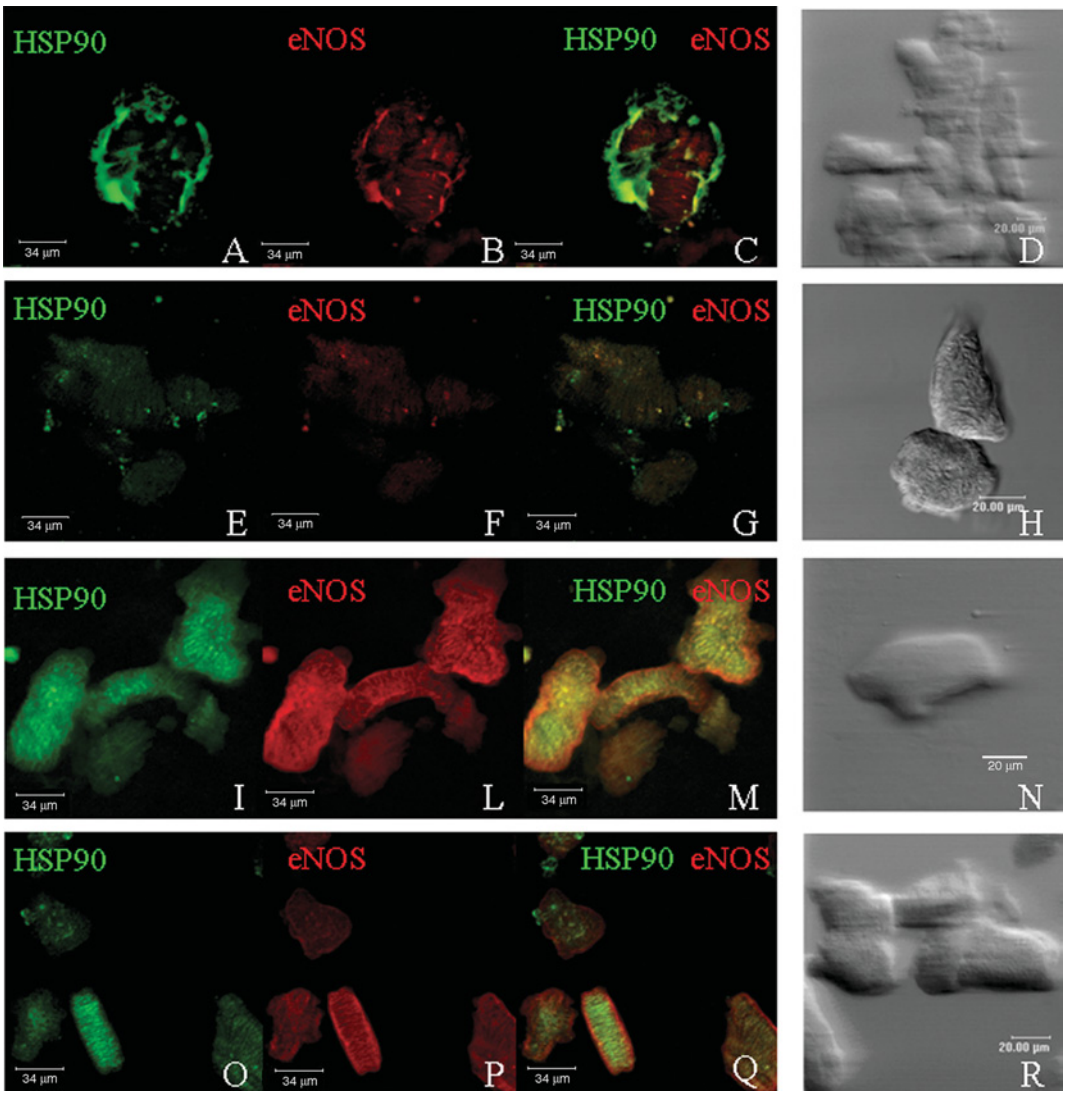

Discussion

Fibronectin, laminin and Matrigel have been suggested as ECM analogues suitable for tissue engineering, due, in large, to their inherent biocompatibility and the fact that they provide a 'blank slate' template upon which key functionalities of the native ECM can be conferred (Hern and Hubbell, 1998; Raeber et al., 2005).

The present work indicates that, whereas monolayer cultures are not satisfactory for cell–ECM interactions, 3D co-cultures or 3D artificial ECM cultures are more suitable for analysing this interaction, since they show a pattern more similar to cardiac tissue. The rapid isolation of cardiomyocytes from the heart ensures the morphological integrity of the cells. Following cardiac tissue disaggregation by collagenase treatment, cells were released from the tissue network. Once released from ECM, the cardiomyocytes maintained their approximate shape, undergoing, however, an internal rearrangement. Although

Figure 4 | HSP90 and eNOS co-localization images obtained by Image J software

Computational overlay representation of red and green signals after background removal is shown (**A**, **C**, **E**, **G**). Pseudocolour PDM images (**B**, **D**, **F**, **H**) showing areas of high and low co-localization (yellow and blue respectively).

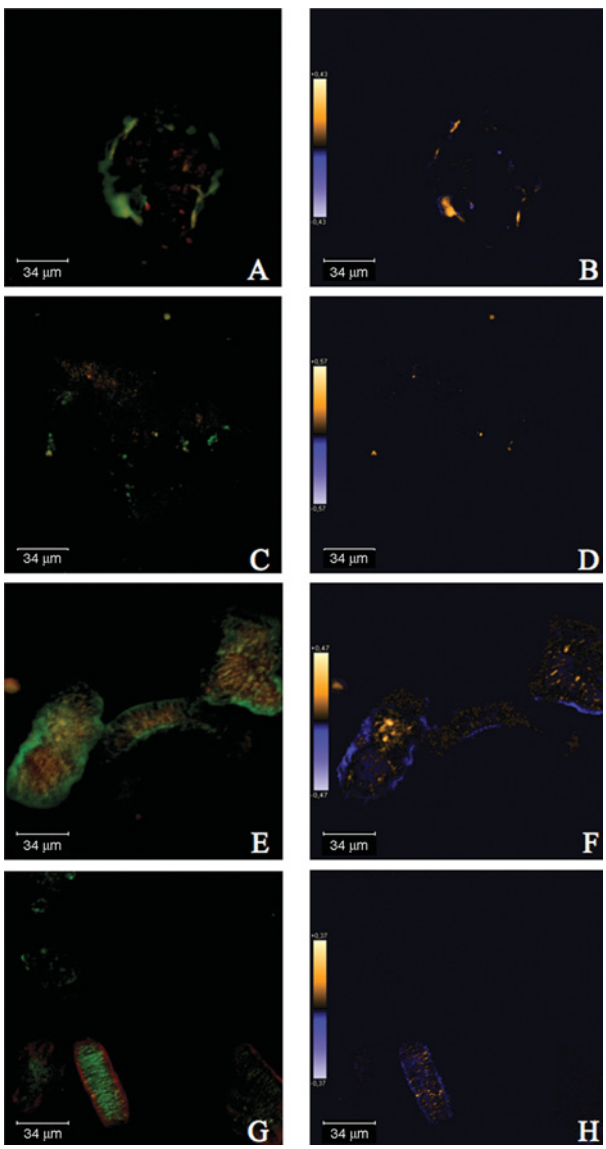

Table 1 | Co-localization coefficients obtained by computational analysis of confocal images

Data from confocal images of cardiomyocytes cultivated on different substrates and incubated with anti-HSP90 and anti-NOS were analysed by the ImageJ software, as shown in Figures 4A–4H (see the Materials and methods section). R_r, $0 \rightarrow 1$, $1 =$ perfect correlation; R, M_1 and M_2, $1 \rightarrow 0$, $1 =$ high co-localization, $0 =$ low co-localization).

	Co-localization coefficient			
Substrate	R_r	R	M_1	M_2
Fibroblast	0.548	0.881	0.767	0.605
Fibronectin	0.621	0.825	0.625	0.499
Matrigel	0.341	0.833	0.975	0.87
Laminin	0.121	0.697	0.599	0.8

some cardiomyocytes maintained the in frame myofibril organization, others did not. These changes are likely due to the absence of the micro-environmental interactions shaping cardiomyocyte cytoarchitecture *in vivo*, as, for example, interactions between sarcomeric and non-sarcomeric cytoskeleton proteins (Ehler and Perriard, 2000) and connections between myofibrils and ECM through integrin/talin-based costameres (Wu et al., 2002).

SEM analysis has revealed important differences among the cultures. In fact, cardiomyocytes cultured on fibronectin and laminin (data not shown) established a poor connection with the substrate. In contrast, SEM micrographs of 3D co-cultures of cardiomyocytes and cardiac fibroblasts showed a strict interaction between the cell types, with cardiac fibroblasts forming an envelope around cardiomyocytes. Matrigel 3D cultures were not suitable for SEM analysis.

TEM morphological analysis of Matrigel 3D cultures showed the integrity of both plasma membrane and intracellular components, such as mitochondria and myofibrils. These morphological features, particularly the integrity of mitochondria, suggest a substantial cell viability of our primary culture preparation. Moreover, these micrographs show that the combined use of sodium cacodylate buffer and L.R. White resin may be useful to save both membranes and cell morphology. The morphological integrity of the isolated cardiomyocytes was confirmed by both the statistical evaluation of cell areas, and by comparing their distribution between 3D cultures and the cardiac tissue. Both samples showed a geometric model of distribution ($P < 0.005$), although the size of cultured cardiomyocytes was half the size of native cardiomyocytes. This indicated that the two different conditions are comparable.

3D cultures were created firstly for the advantage they provided for cancer research, since they reproduce the invasive behaviour of tumour cells (Kim et al., 2004; Kim, 2005). Many methods have been

developed, but most of them are not suitable for immobile non-dividing cells, such as cardiomyocytes. Rotary cell culture systems, pre-engineered scaffolds, gyratory and spinner flasks, and liquid overlay cultures cannot be used with cardiomyocytes, since they favour cardiac fibroblasts accumulation and proliferation, together with altered ECM production (Kim et al., 2004; Kim, 2005). Pure matrices and ECM components, as used in our 3D system, may overcome these problems and, embedding the entire cell, may favour the development of cell–ECM interactions. This allows our culture system to be utilized for both 3D high-resolution second-harmonic generation imaging in polarization studies on artificial matrices molecular organization and symmetry (Campagnola et al., 2002). Interestingly, under the cultural conditions developed in our study, cardiomyocytes survive for up to 5 days (data not shown). This makes our cultures suitable for time-lapse confocal microscopy on living cells, which can probe the function of macromolecules in their natural environment, with ever increasing spatial and temporal resolution (Pepperkok and Ellenberg, 2006).

Once we had validated our cultural systems, we used 3D-cultured cardiomyocytes to study subcellular localization and co-localization of the two correlated proteins HSP90 and eNOS. Confocal laser-scanning microscopy revealed HSP90 and eNOS expression in all cell cultures. However, as revealed by the different localization of the fluorescent signal, their expression changed qualitatively depending on the substrate. In fact, in cardiomyocytes cultured on fibronectin as a monolayer, HSP90 and eNOS signals were concentrated in small spots within the cell. In cardiomyocytes co-cultured with cardiac fibroblasts, although HSP90 appeared to be mainly localized close to the cell membrane, the intimate interaction between fibroblasts and cardiomyocytes did not allow cell type in which the signal was located to be clearly discriminated. In contrast, in cardiomyocytes cultured embedded either in Matrigel, or in laminin, HSP90 labelling was located in the cytoplasm. HSP90 is an ubiquitous protein expressed at high levels (accounting for up to 1–2% of total cellular protein content) in the cytosol, even in unstressed conditions (Obermann et al., 1998), and may act both as a chaperone and docking protein in different signalling pathways also found in cardiac cells. We suggest that the variable HSP90 compartmentalization observed in our four different culture systems depends on the ECM component used as a substrate.

eNOS also appeared to differently localize within cardiomyocytes depending on the substrate used to culture the cells. On fibronectin, cultured myocytes express a low level of eNOS, which is detected as small spots randomly located within the cells. On the contrary, in cardiomyocytes cultured on Matrigel or laminin, or in co-culture with fibroblasts, a definite eNOS immunofluorescence signal associates with the sarcolemma. As for HSP90 expression, in co-cultures, the large association between cardiomyocytes and fibroblasts did not allow cell type in which the signal was located to be clearly discriminated. The distribution pattern of eNOS observed in Matrigel cultures agrees with the prevalent enzyme subcellular compartmentalization described in mammalian atrial and ventricular cardiomyocytes (Barouch et al., 2002; Massion et al., 2005). In these cells, eNOS is targeted to caveolin-3 at the plasma membranes, and possibly in T-tubular membranes as well (Massion et al., 2005). Such a membrane spatial restriction contributes to regulate enzyme activity. In fact, disruption of caveolin-3 binding, allows eNOS to be activated via AKT-dependent phosphorylation (Fulton et al., 1999). This requires HSP90 synergistic recruitment (Takahashi and Mendelsohn, 2003). Association with HSP90 may also prevent eNOS uncoupling, i.e. its production of superoxide anions instead of NO (Pritchard et al., 2001). In addition, eNOS activity is regulated by the association with both integrins and other molecules involved in cell adhesion [i.e. FAK (focal adhesion kinase)], which link eNOS to the PI3K/AKT (phosphoinositide 3-kinase/AKT) pathway (Gallis et al., 1999). This multitude of molecular associations permit eNOS to rapidly respond to extracellular signals (i.e. fluid shear stress, oxygen, growth factors and hormones) (Garcia-Cardena et al., 1998; Brouet et al., 2001), not only under physiological conditions, but also under physio-pathological alterations, including hypoxia, ischaemia/reperfusion injuries and hypertrophy (Piech et al., 2003; Kupatt et al., 2004). Interestingly, our co-localization studies on laminin and, above all, on Matrigel-cultured cardiomyocytes, revealed sites characterized by the simultaneous presence of eNOS and HSP90. This agrees with the results of immunolabelling studies which have revealed the two proteins to be co-localized (Khurana et al., 2000; Venema

et al., 2003). Accordingly, these two substrates can be regarded as potentially suitable to obtain a high expression and an appropriate subcellular compartmentalization of the two proteins, thus reproducing a condition close to that encountered in *in vivo* cells. On the contrary, cardiomyocytes cultured with either cardiac fibroblasts or on fibronectin show limited expression and correlation between the two proteins. Literature has demonstrated that fibroblasts, which contaminate both fibronectin (2D) and collagen (3D) cultures of cardiomyocytes, synthesize and secrete humoral factors [for example, bFGF (basic fibroblast growth factor)] which are able to influence not only cell morphology, but also the expression of proteins such as α-SM-1 (α smooth muscle 1) actin or troponin (van Luyn et al., 2002). We hypothesize that the reduction of both HSP90 and eNOS observed in our co-cultured cardiomyocytes may be influenced by fibroblast-released proteins.

In conclusion, our 3D adult cardiomyocyte culture system, in combination with the method of epitope-tagging of signalling proteins, appears to be ideally suited to monitor the impact of the biochemical micro-environment on the cardiomyocyte phenotype. Our system allows a correlation between ECM components and cellular localization of proteins, which are not directly involved in integrin outside–in signalling, to be revealed. Accordingly, it represents a testable model for either living or fixed cells for analysing, in a 3D architectural context, the molecular interactions between cardiomyocytes and ECM.

Methods

Isolation of adult rat cardiomyocytes

Cardiomyocytes were obtained from 3-month-old female Sprague–Dawley rats (150–200 g) by aseptic dissection and treatment of heart ventricles with collagenase type II (50 units/ml) and 1.25 mmol/l $CaCl_2$ in HBSS (Hanks balanced salt solution) for 90 min. Rats were anaesthetized with 2% haloethane in O_2. All the experiments on animals were performed in accordance with 'Ministero della Salute' guidelines for animal experimentation. After treatment (6 h), freshly dissociated cells were filtered through an 80 μm mesh (Millipore), washed by centrifugation at 500 rev./min and resuspended in M-199 medium (Sigma–Aldrich) supplemented with 20% FBS (foetal bovine serum; Biolife), 1 μg/ml fungizone, 100 μg/ml streptomycin and 100 units/ml penicillin. The cell suspension was then subjected to a 24 h period of differential adhesion to separate two different populations of cells: cardiomyocytes in suspension and cardiac fibroblasts adherent to plastic ware. At the end of the differential adhesion interval period, myocytes obtained from a single heart were concentrated by centrifugation and maintained in culture in suspension in 75-cm^2 flasks in M-199 medium/20% FBS, and cardiac fibroblasts were maintained in culture in 75-cm^2 flasks in monolayers in M-199 medium/20% FBS. For monolayer experiments cardiomyocytes were plated on to BD Falcon 24-well-plates inserts (3×10^4) or 8-well chamberslides (5×10^3) on mouse plasma fibronectin (5 μg/ml) or mouse laminin (5 μg/ml) (Gibco).

3D culture design

3D cultures in artificial ECM were generated using BD Matrigel basement membrane (growth-factor reduced, mouse, natural) as substrate. For Matrigel gels, cardiomyocytes were embedded in a solution of Matrigel diluted 1:3 in M-199 medium /20% FBS, as indicated by the manufacturer. These components formed a 3D gel matrix within 30 min. Gels were superfused with M-199 medium/20% FBS and placed in a cell culture incubator (95% O_2/5% CO_2, 37°C). After plating (24 h), cells were fixed and used for TEM or confocal laser-scanning microscopy.

3D co-cultures with cardiac fibroblasts were generated by plating cardiomyocytes on a monolayer of cardiac fibroblasts plated 24 h before on BD inserts or chamberslides. Co-cultures were then fixed and used for either SEM or confocal laser-scanning microscopy.

SEM of 3D-cardiomyocyte-cultures

Isolated rat cardiomyocytes were prepared for SEM analysis to analyse cell morphology and attachment capacity. Cells, grown on BD Falcon inserts for 24-well plates on the appropriate substrate, were rinsed with phosphate buffer (pH 7.3) to remove medium and then fixed in 2.5% glutaraldehyde in phosphate buffer (pH 7.3). Samples were rinsed again in phosphate buffer (pH 7.3) and post-fixed in 1% osmium tetroxide in the same buffer for 1 h. After dehydration with graded ethanol (30%, 50%, 70%, 95% and 100%), samples were critically point-dried with CO_2, mounted on specimen stubs and sputter-coated with gold particles. SEM examination was performed at 15 (30) kV emission voltage on a JSM-6301F scanning microscope.

TEM

Cardiomyocytes (3×10^4 per well), 48 h after isolation, were mixed with 50 μl of liquid Matrigel on ice, seeded into BD Falcon inserts for 24-well plates with translucent membranes and left to solidify at 37°C. After plating (24 h), cultures were fixed with 4% paraformaldehyde and 0.05% glutaraldehyde in 100 mM sodium cacodylate buffer (pH 7.4) for 30 min and included the same day.

Ventricles from 3-month-old (150–200 g) female Sprague–Dawley rats were cut into 1 mm pieces, fixed into 4% paraformaldehyde and 0.05% glutaraldehyde in 100 mM sodium cacodylate buffer (pH 7.4) for 1 h and included the same day. After fixation, samples were rinsed twice with 100 mM sodium cacodylate buffer (pH 7.4), dehydrated with ethanol (30%, 50% and 70%). After dehydration cells were embedded into L.R. White resin with passages of 1:3 of resin/70% ethanol, 3:1 resin/70% ethanol, pure resin for 1 h, pure resin overnight, pure resin 1 h before inclusion at 50°C for 48 h. The day after, another passage with resin only was done and, finally, the membranes of the inserts were included into gelatin capsules with the bottom up, to allow the plastic membrane to be peeled away after inclusion. Semi-thin sections were obtained and stained with Methylene Blue.

Confocal laser-scanning microscopy

For confocal laser-scanning microscopy, 3D cardiomyocyte cultures were set in 8-well chamberslides. To limit artifacts and to compare the immunofluorescence intensity between the four substrates and the different cultural conditions, each set of experiments was done with the same cell preparation and immunofluorescence experiments were performed simultaneously. Moreover, during confocal microscope observations, all parameters for picture acquisition were kept the same and automatically saved. This analysis permitted the 3D study of intracellular protein localization. After plating (24 h), cells were fixed with 2.5% paraformaldehyde in PBS for 30 min and ice-cold methanol for 30 min, and were blocked with 5% BSA in PBS and incubated with the first primary antibody overnight (1:50, anti-HSP90α/β; Santa Cruz Biotechnology catalogue no. SC-13119), and with the second primary antibody overnight the day after (1:50, anti-eNOS; Sigma–Aldrich catalogue no. 3893). After washing with PBS, cells were further incubated with fluorescent secondary antibodies (1:50, FITC-conjugated anti-mouse secondary antibody, Amersham Biosciences; 1:50, TRITC-conjugated anti-mouse secondary antibody, Sigma–Aldrich; 1:50, FITC-conjugated anti-rabbit secondary antibody, Sigma–Aldrich; 1:50, Texas Red-conjugated secondary antibody, Amersham Biosciences). Double-staining immunofluorescence experiments were performed with green anti-mouse/red anti-rabbit and vice versa, as a control. For imaging, a Leica laser-scanning confocal microscope was used. Scanning analysis was performed with Leica analysis software.

Statistical analysis

To compare cell area distributions between heart tissue and 3D cultures of cardiomyocytes, cell areas were measured on 10 semithin sections of L.R. White resin inclusions of heart tissue and 3D cultures. Cell areas were measured on 10 regions per section, using the cell area measurement plug-in of the ImageJ software (http://rsb.info.nih.gov/ij/). Cell area distribution analyses were performed using Statistica 6.0 for Windows XP.

Co-localization was determined with the ImageJ intensity correlation analysis plug-in. Two images of each substrate (HSP90 in green and eNOS in red) were analysed, obtaining four images. Specifically, two of them showed HSP90 and eNOS localization after background removal for both the red and green channels respectively. A third image was an overlay of both red and green signals; a fourth pseudocolour PDM [PDM for each pixel = (red intensity−mean red intensity) × (green intensity−mean green intensity)] image showed in yellow and in blue the areas of high and low co-localization respectively, and in black the areas without correlation between the two proteins. The plug-in also provided the R_r value (ranging between 0 and 1, where 1 is perfect correlation), the R value (ranging between 1 and 0, where 1 is high and 0 is low co-localization), the M_1 and M_2 values, and a co-localization PDM image in which blue and yellow correspond to absence and presence of co-localization respectively.

Acknowledgements

This study was supported by the Ministero dell'Istruzione, dell'Università e della Ricerca Scientifica (ex 60%, 2004) and Progetti di Rilevante Interesse Nazionale (PRIN) (2003).

References

Aoyagi, Y., Fujita, N. and Tsuruo, T. (2005) Stabilization of integrin-linked kinase by binding to Hsp90. Biochem. Biophys. Res. Commun. **331**, 1061–1068

Barouch, L.A., Harrison, R.W., Skaf, M.W., Rosas, G.O., Cappola, T.P., Kobeissi, Z.A., Hobai, I.A., Lemmon, C.A., Burnett, A.L., O'Rourke, B., Rodriguez, E.R., Huang, P.L., Lima, J.A., Berkowitz, D.E. and Hare, J.M. (2002) Nitric oxide regulates the heart by spatial confinement of nitric oxide synthase isoforms. Nature **416**, 337–339

Brouet, A., Sonveaux, P., Dessy, C., Moniotte, S., Balligand, J.L. and Feron, O. (2001) Hsp90 and caveolin are key targets for the proangiogenic nitric oxide-mediated effects of statins. Circ. Res. **89**, 866–873

Campagnola, P.J., Millard, A.C., Terasaki, M., Hoppe, P.E., Malone, C.J. and Mohler, W.A. (2002) Three-dimensional high-resolution second-harmonic generation imaging of endogenous structural proteins in biological tissues. Biophys. J. **82**, 493–508

Ehler, E. and Perriard, J.C. (2000) Cardiomyocyte cytoskeleton and myofibrillogenesis in healthy and diseased heart. Heart Fail. Rev. **5**, 259–269

Eisenberg, L.M. and Eisenberg, C.A. (2004) Adult stem cells and their cardiac potential. Anat. Rec. A. Discov. Mol. Cell. Evol. Biol. **276**, 103–112

Fulton, D., Gratton, J.P., McCabe, T.J., Fontana, J., Fujio, Y., Walsh, K., Franke, T.F., Papapetropoulos, A. and Sessa, W.C. (1999) Regulation of endothelium-derived nitric oxide production by the protein kinase Akt. Nature **399**, 597–601

Gallis, B., Corthals, G.L., Goodlett, D.R., Ueba, H., Kim, F., Presnell, S.R., Figeys, D., Harrison, D.G., Berk, B.C., Aebersold, R. and Corson, M.A. (1999) Identification of flow-dependent endothelial nitric-oxide synthase phosphorylation sites by mass spectrometry and regulation of phosphorylation and nitric oxide production by the phosphatidylinositol 3-kinase inhibitor LY294002. J. Biol. Chem. **274**, 30101–30108

Garcia-Cardena, G., Fan, R., Shah, V., Sorrentino, R., Cirino, G., Papapetropoulos, A. and Sessa, W.C. (1998) Dynamic activation of endothelial nitric oxide synthase by Hsp90. Nature **392**, 821–824

Griffith, L.G. and Naughton, G. (2002) Tissue engineering – current challenges and expanding opportunities. Science **295**, 1009–1014

Hern, D.L. and Hubbell, J.A. (1998) Incorporation of adhesion peptides into non-adhesive hydrogels useful for tissue resurfacing. J. Biomed. Mater. Res. **39**, 266–276

Imanaka-Yoshida, K., Enomoto-Iwamoto, M., Yoshida, T. and Sakakura, T. (1999) Vinculin, talin, integrin $\alpha6\beta1$ and laminin can serve as components of attachment complex mediating contraction force transmission from cardiomyocytes to extracellular matrix. Cell Motil. Cytoskeleton **42**, 1–11

Jacobson, S.L., Kennedy, C.B. and Mealing, G.A. (1983) Evidence for functional sodium and calcium ion channels in the membrane of cultured cardiomyocytes of the adult rat. Can. J. Physiol. Pharmacol. **61**, 1312–1316

Khurana, V.G., Feterik, K., Springett, M.J., Eguchi, D., Shah, V. and Katusic, Z.S. (2000) Functional interdependence and colocalization of endothelial nitric oxide synthase and heat shock protein 90 in cerebral arteries. J. Cereb. Blood Flow Metab. **20**, 1563–1570

Kim, J.B. (2005) Three-dimensional tissue culture models in cancer biology. Semin. Cancer Biol. **15**, 365–377

Kim, J.B., O'Hare, M.J. and Stein, R. (2004) Models of breast cancer: is merging human and animal models the future? Breast Cancer Res. **6**, 22–30

Kupatt, C., Dessy, C., Hinkel, R., Raake, P., Daneau, G., Bouzin, C., Boekstegers, P. and Feron, O. (2004) Heat shock protein 90 transfection reduces ischemia–reperfusion-induced myocardial dysfunction via reciprocal endothelial NO synthase serine 1177 phosphorylation and threonine 495 dephosphorylation. Arterioscler. Thromb. Vasc. Biol. **24**, 1435–1441

Massion, P.B., Pelat, M., Belge, C. and Balligand, J.L. (2005) Regulation of the mammalian heart function by nitric oxide. Comp. Biochem. Physiol., Part A Mol. Integr. Physiol. **142**, 144–150

Matsushita, T., Oyamada, M., Fujimoto, K., Yasuda, Y., Masuda, S., Wada, Y., Oka, T. and Takamatsu, T. (1999) Remodeling of cell–cell and cell–extracellular matrix interactions at the border zone of rat myocardial infarcts. Circ. Res. **85**, 1046–1055

Nag, A.C., Cheng, M., Fischman, D.A. and Zak, R. (1983) Long-term cell culture of adult mammalian cardiac myocytes: electron microscopic and immunofluorescent analyses of myofibrillar structure. J. Mol. Cell. Cardiol. **15**, 301–317

Nerem, R.M. and Seliktar, D. (2001) Vascular tissue engineering. Annu. Rev. Biomed. Eng. **3**, 225–243

Niklason, L.E. (1999) Techview: medical technology. Replacement arteries made to order. Science **286**, 1493–1494

Obermann, W.M., Sondermann, H., Russo, A.A., Pavletich, N.P. and Hartl, F.U. (1998) *In vivo* function of Hsp90 is dependent on ATP binding and ATP hydrolysis. J. Cell Biol. **143**, 901–910

Pepperkok, R. and Ellenberg, J. (2006) High-throughput fluorescence microscopy for systems biology. Nat. Rev. Mol. Cell. Biol. **7**, 690–696

Peyton, S.R., Raub, C.B., Keschrumrus, V.P. and Putnam, A.J. (2006) The use of poly(ethylene glycol) hydrogels to investigate the impact of ECM chemistry and mechanics on smooth muscle cells. Biomaterials **27**, 4881–4893

Piech, A., Dessy, C., Havaux, X., Feron, O. and Balligand, J.L. (2003) Differential regulation of nitric oxide synthases and their allosteric regulators in heart and vessels of hypertensive rats. Cardiovasc. Res. **57**, 456–467

Pritchard, Jr, K.A., Ackerman, A.W., Gross, E.R., Stepp, D.W., Shi, Y., Fontana, J.T., Baker, J.E. and Sessa, W.C. (2001) Heat shock protein 90 mediates the balance of nitric oxide and superoxide anion from endothelial nitric-oxide synthase. J. Biol. Chem. **276**, 17621–17624

Raeber, G.P., Lutolf, M.P. and Hubbell, J.A. (2005) Molecularly engineered PEG hydrogels: a novel model system for proteolytically mediated cell migration. Biophys. J. **89**, 1374–1388

Sharp, W.W., Simpson, D.G., Borg, T.K., Samarel, A.M. and Terracio, L. (1997) Mechanical forces regulate focal adhesion and costamere assembly in cardiac myocytes. Am. J. Physiol. **273**, H546–H556

Takahashi, S. and Mendelsohn, M.E. (2003) Synergistic activation of endothelial nitric-oxide synthase (eNOS) by HSP90 and Akt: calcium-independent eNOS activation involves formation of an HSP90–Akt–CaM-bound eNOS complex. J. Biol. Chem. **278**, 30821–30827

Tota, B., Quintieri, A.M., Di Felice, V. and Cerra, M.C. (2007) New biological aspects of chromogranin A-derived peptides: focus on vasostatins. Comp. Biochem. Physiol., Part A Mol. Integr. Physiol. **147**, 11–18

van Luyn, M.J., Tio, R.A., Gallego y van Seijen, X.J., Plantinga, J.A., de Leij, L.F., DeJongste, M.J. and van Wachem, P.B. (2002) Cardiac tissue engineering: characteristics of in unison contracting two- and three-dimensional neonatal rat ventricle cell (co)-cultures. Biomaterials **23**, 4793–4801

VanWinkle, W.B., Snuggs, M.B., De Hostos, E.L., Buja, L.M., Woods, A. and Couchman, J.R. (2002) Localization of the transmembrane proteoglycan syndecan-4 and its regulatory kinases in costameres of rat cardiomyocytes: a deconvolution microscopic study. Anat. Rec. **268**, 38–46

Venema, R.C., Venema, V.J., Ju, H., Harris, M.B., Snead, C., Jilling, T., Dimitropoulou, C., Maragoudakis, M.E. and Catravas, J.D. (2003) Novel complexes of guanylate cyclase with heat shock protein 90 and nitric oxide synthase. Am. J. Physiol. Heart Circ. Physiol. **285**, H669–H678

Willey, C.D., Balasubramanian, S., Rodriguez Rosas, M.C., Ross, R.S. and Kuppuswamy, D. (2003) Focal complex formation in adult cardiomyocytes is accompanied by the activation of β3 integrin and c-Src. J. Mol. Cell. Cardiol. **35**, 671–683

Wu, J.C., Sung, H.C., Chung, T.H. and DePhilip, R.M. (2002) Role of N-cadherin- and integrin-based costameres in the development of rat cardiomyocytes. J. Cell. Biochem. **84**, 717–724

Received 5 April 2007/30 May 2007; accepted 28 June 2007

Published as Immediate Publication 28 June 2007, doi:10.1042/BC20070043